

Study and Modelling of the Thermo-mechanical Behaviour of Melt-textured YBaCuO-composites Containing Ag and/or 211 Particles

F. Tancret,^{ab†} J.-M. Haussonne,^c I. Monot,^a O. Vansse^b and F. Osterstock^{b*}

^aISMRA and CRISMAT, 6 Bd. du Maréchal Juin, F-14050 Caen Cedex, France

^bISMRA and LERMAT, 6 Bd. du Maréchal Juin, F-14050 Caen Cedex, France

^cEcole D'Ingénieurs de Cherbourg, F-50130 Octeville, France

Abstract

YBa₂Cu₃O_x high-T_c ceramic superconductors have been elaborated by the melt-textured-growth method with additions of Ag particles and/or Y₂BaCuO₅ (211 green phase) in order to study the fracture properties and the thermal shock resistance. The Vickers indentation technique, initially devoted to the sole determination of the toughness has been used in conjunction with a new thermal shock resistance parameter. It makes use of the initial stage of stable propagation of Vickers indentation cracks when submitted to a thermal stress, and results in a generalisation of the fourth parameter of Hasselman. Whereas the toughness increases with increasing 211 content, does the thermal shock resistance decrease. This is explained with respect of the strongly micro-cracked (along the 001 planes) microstructure which is seen as a stacking of dense laminates bound by the 211 particles and subjected to a linear temperature gradient. The higher the number of bounding particles, the stiffer the quenched material, and the higher the induced thermal stress. This micro-mechanical model is implemented into a finite element software. The first results of the calculations confirm the above approach. © 1999 Elsevier Science Limited. All rights reserved

Keywords: composites, thermal shock resistance, toughness and toughening, oxide superconductors.

1 Introduction

The use of YBa₂Cu₃O_x, (123) ceramic superconductors below their critical temperature includes cooling or quenching the parts to the temperature of liquid nitrogen (T_b^o = 77 K), which may lead to macroscopic crack extension under the action of the transient thermal stress. The increased temperature difference, with respect to that of the elaboration, provokes additionally an increase of the residual thermal mismatch stresses of the second kind, which are due to the anisotropy of the coefficients of thermal expansion. They may induce severe micro-cracking resulting in a decrease of the super-conducting current transport properties. A need for improved thermal shock resistance appears thus. This is worked-out within the competition between the thermal transient stress due to quenching and the toughness (crack extension) of the material. The main parameters of a quenching system have been reviewed by Kingery¹ and Buessem.² The methodology is to increase the toughness and to achieve the highest thermal conductivity to lower the thermal transient stress. It can be made with the use of composite effects as for the case of polycrystalline bodies. Due to the peritectic decomposition, the Y₂BaCuO₅ (the green 211) phase nucleates in the textured microstructure, and its amount can be monitored. The measurement of the toughness can be realised by using the Vickers indentation technique.^{3–5} Furthermore, does the stage of stable crack extension of the Vickers indentation cracks under the action of the transient thermal stress 'freeze-in' its maximum value and thus allow quantitative comparisons. The apparent discrepancies are worked-out

*To whom correspondence should be addressed. Fax: +33-231-452673; e-mail: osterstock@labolermat.ismra.fr

†Present address: Department of Materials Science and Metallurgy, University of Cambridge, UK.

within the frame of a meso-structural model that can be implemented into a finite element software.

2 Experimental

The investigated materials are platinum-doped (0.5% PtO₂), top-seeded and melt-textured YBa₂CuO_x/Y₂BaCuO₅ (123/211) and YBa₂CuO₃O_x/Y₂BaCuO₅/Ag (123/211/Ag), composites. The samples are discs (diameter: 20 mm, height: 6.5 mm) of quasi-single crystals containing trapped 211 and silver particles, 5 and 20 μm in diameter, respectively. Vickers indentations, with several loads between 4.9 to 300 N, have been introduced on the polished surfaces, corresponding to the 123 (001) planes. The initial (after indentation) and resulting (after quenching) lengths, c_0 and c , respectively, of the radial cracks have been measured with an eye-piece having a resolution of 1 μm.

3 Results

3.1 Toughness and thermal shock resistance

The toughness, K_c , of the material has been calculated using the relation derived by Chantikul *et al.*⁶ for the case of median-radial cracks, of length, c_0 , due to a Vickers indentation of load, P ,

$$K_c = \chi_r \cdot P \cdot c_0^{-3/2} \quad (1)$$

where χ_r is a constant equal to 0.1 in the case of dense YBa₂Cu₃O_x ceramics.⁴ The values of K_c are plotted in Fig. 1 as a function of the content of 211 particles. The value K_c for the 123 single crystal⁷ is also given. Up to 50% mol, the presence of the

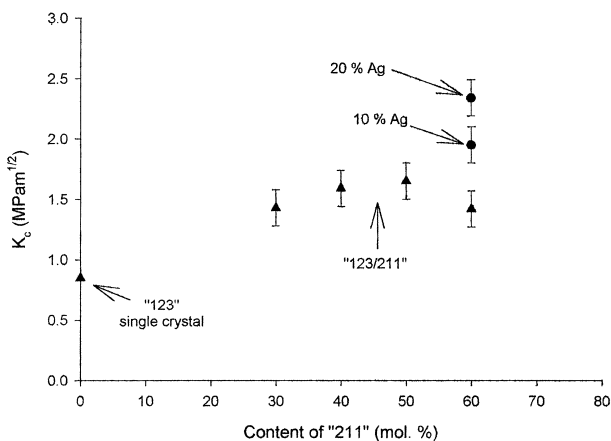


Fig. 1. Toughness, K_c , of a textured super-conducting YBa₂Cu₃O_x matrix reinforced by the ceramic 211-green-phase particles and by silver particles for 60% mol content of 211. With respect to the toughness of the single crystal,⁷ an increase of that material property can be observed. The error bars are due to the scatter in the crack-length.

211 particles provokes a marked increase of the toughness in a first step. The observed micro-mechanism of crack extension is deflection by the residual mismatch stress field around the 211 particles. When the amount becomes too high (60% mol), this toughening mechanism becomes less efficient, probably as a result of interactions between stress fields. When submitted to a mechanical or thermal stress, the radial indentation cracks propagate first in a stable way under the combined action of the residual contact stresses and the applied stress. Their relative extension, from c_0 to the actual value, c , thus 'freezes-in' the maximum value of the thermal transient stress, σ_{th} , due to quenching. This is given by the following:

$$K_c = \chi_r \cdot P \cdot c_0^{-3/2} = \chi_r \cdot P \cdot c^{-3/2} - \sigma_{th}(\pi\Omega c)^{1/2} \quad (2)$$

where Ω is the geometrical factor for a semi-elliptical surface crack ($\Omega = 4/\pi^2$). The thermal shock resistance parameter $R_{th} = (K_c/\sigma_{th})^2$ describes the competition between the toughness of the material and the thermal transient stress. It results in:⁵

$$R_{th} = (\pi\Omega c)/(1 - (c/c_0)^{-3/2})^2 \quad (3)$$

The disc-shaped textured samples were fitted with several indentations under different loads and the initial lengths, c_0 , of the radial cracks measured (see Fig. 3). The sample is then quenched into liquid nitrogen ($\Delta T = 300$ K), removed and allowed to reheat within water absorbing paper to avoid stress enhanced corrosion. In order to achieve a more severe thermal shock, quenching was also realised in first heating the indented sample to 320°C and dropping it into low viscosity silicon oil at room temperature ($\Delta T = 300$ K, also). The resulting crack lengths were then measured and the thermal shock resistance parameter, R_{th} , deduced from the slope of the c versus $(1 - (c/c_0)^{-3/2})^2$ plot. From a physical point of view, R_{th} indicates relative thermal shock resistances of different materials at quenching temperature differences, ΔT , lower than the classical ΔT_c . The values for toughness and thermal shock resistance (quenching into silicon oil) are listed in Table 1. The variation of R_{th} with 211 is plotted in Fig. 2. The increase of R_{th} due to the addition of Ag is much larger and was not plotted because largely out of scale. It reflects the effect of silver in increasing the thermal conductivity, thus lowering the thermal transient stress.

For the case of the 123/211 composites, the toughness increases with increasing amount of 211 particles, whereas the thermal shock resistance

Table 1. Microstructural characteristics and thermo-mechanical properties of the materials used in the experiments (the values of R_{th} are those resulting from quenching into silicon oil)

123:211 stoichiometry (211 adjunction, mol%)	Silver volume fraction (%)	Toughness (K_c) ($MPa m^{1/2}$)	R_{th} (mm) silicon oil ($\Delta T = 300 K$)
1:0.3 (30)	0	1.43	3.05
1:0.4 (40)	0	1.59	2.04
1:0.5 (50)	0	1.65	1.36
1:0.6 (60)	0	1.42	—
1:0.6 (60)	10	1.95	—
1:0.6 (60)	20	2.34	—

decreases at the same time. This indicates that the induced thermal stress increases more with increasing 211-content than does toughness. The later can be described by the effect of crack deflection mechanisms due to the elastic and thermal mismatch stresses around the 211-particles, and reveals to be rather narrow.⁸ An increase of the maximum of the thermal transient stress during quenching must be proposed and justified.

3.2 Microstructural and micro-mechanical modelling

Assuming that neither the Young's modulus nor the thermal conductivity would be changed by the presence of the 211-particles, the classical theories for dense and isotropic bodies would predict an increase in thermal shock resistance because the toughness increases with the 211-content. The microscopic observation of the textured parts reveals also that these textured samples are strongly micro-cracked along the 123 (001) planes.

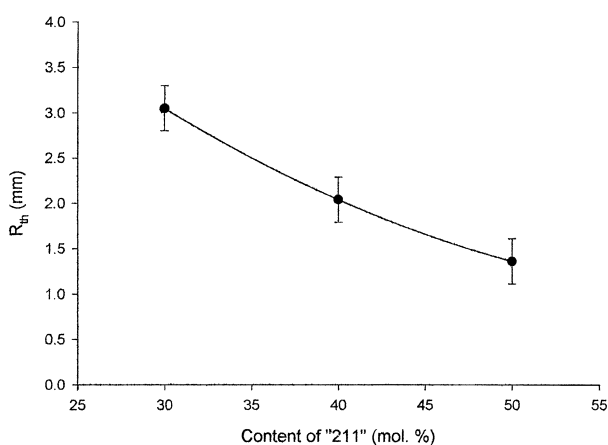


Fig. 2. Thermal shock resistance parameter, R_{th} , of the superconducting $YBa_2Cu_3O_x$ -matrix reinforced by solely the ceramic 211-green-phase-particles as a function of their amount. The values result from quenching the indented samples (pre-heated to 320°C in air) into silicon oil at room temperature. The temperature difference, $\Delta T = 300 K$ is then the same as in quenching from room temperature, in air, into liquid nitrogen. Due the difference in heat transfer the quench test into silicon oil (forced or natural convection) is much harder than that into liquid nitrogen (boiling film).

According to these observations, the microstructure can be represented by a stacking of dense laminates which are bound by the 211 inclusions. The scheme is shown in Fig. 3. The assumed linear temperature gradient, from T_{core} , at the interior, to T_i , temperature of the quenching medium, at the exterior of the sample, is also sketched. The cylinder external walls, perpendicular to the 001-planes are not considered here because the highest transient thermal stress occurs on the basis.

Basic principles can thus be applied to that meso-structural model. An isotropic plate submitted to a linear temperature gradient across its section and deforming freely will not give rise to a thermal stress. By extension it is considered as being the case of the stacking of laminates as long as they are not bound (absence of 211-particles). If they are (presence of 211-particles), they are not longer allowed to deform freely and a thermal stress will build up under the action of the temperature gradient during quenching. The higher the number of 211-particles, the stiffer will be the quenched body and the higher the induced thermal stress. The extreme case is that of completely sticking laminates. They would then behave like a dense and un-cracked bulk. The drop of the thermal shock resistance parameter, R_{th} , results thus from the increase in thermal stress, due to the stiffening effect of the increased number of bonds by 211-particles, which results in an increase of the thermal stress larger than that of toughness.

This meso-structural model has been implemented into a finite element software (Castem 2000). Although it does not strictly respond the anisotropic characteristics of $YBa_2Cu_3O_x$, it has

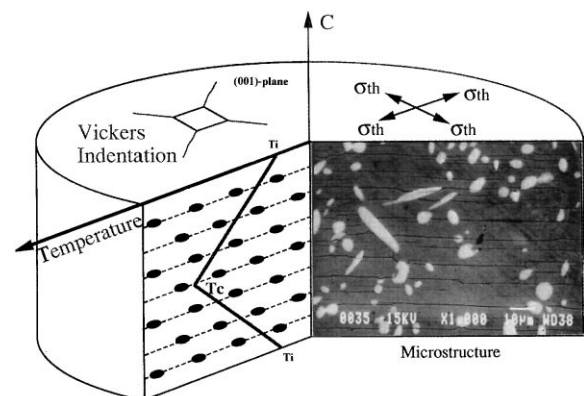


Fig. 3. Micro-graphical view of the 211 reinforced 123-matrix (on the right-hand), and its meso-structural modelling (on the left hand). The cracks in the 123-matrix arise from the strong crystallographic anisotropy in the thermal expansion coefficients. These cracks are bridged by sticking 211-particles which are white on the photograph. The linear temperature gradient ($\Delta T = 300 K$) is also sketched. The Vickers indentation were introduced onto the (001)-plane with an orientation to make the radial cracks perpendicular to the expected radial and tangential stresses appearing in the quenched disc.

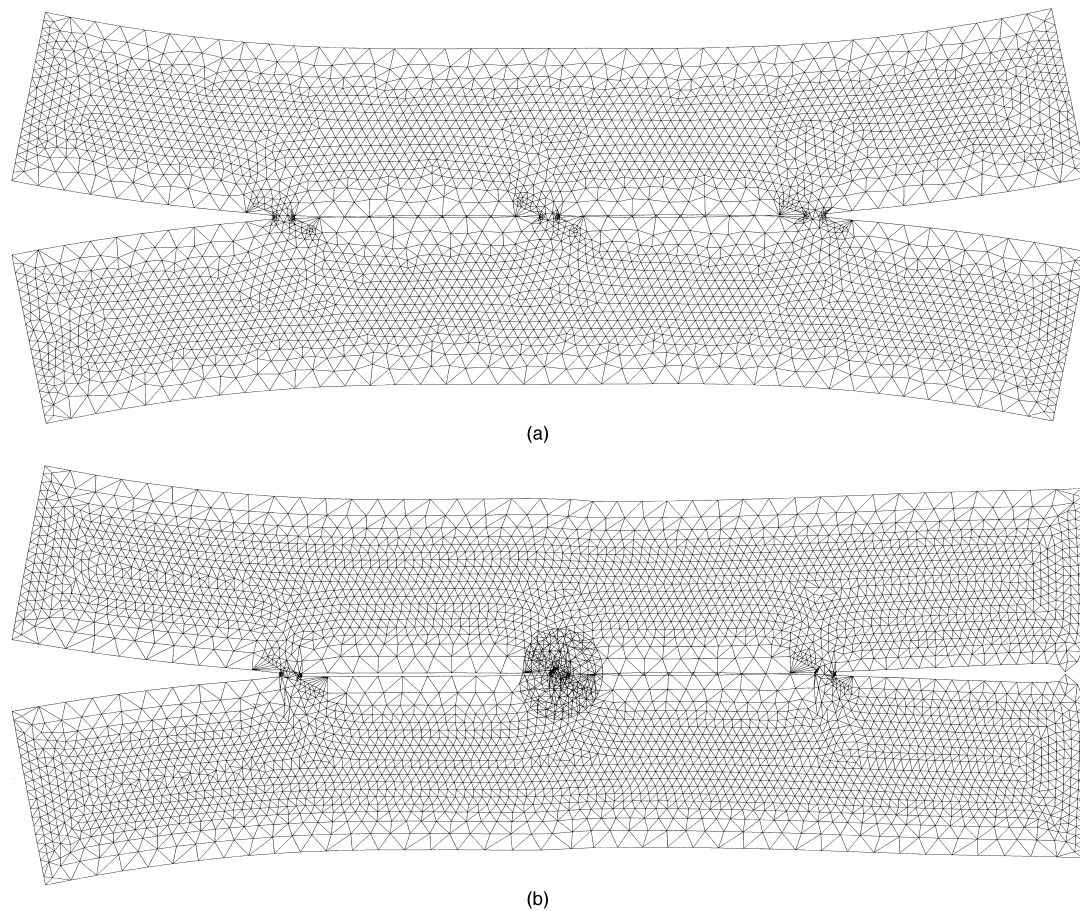


Fig. 4. Views of the finite element simulation (Castem 2000) of the deformed meshing resulting from the numerical imposition of a linear temperature gradient of $\Delta T = 300$ K across each laminate and representing the microstructural modelling of the textured samples. (a) two dense laminates are stuck by three 211 inclusions; (b) Two dense laminates are stuck by an additional 211 inclusion.

been assumed in this first step that the Young's modulus and the coefficient of thermal expansion are isotropic. The deformations of the meshing are represented in Fig. 4. In a first step two lamellae are bound by three inclusions. The linear temperature gradient of $\Delta T = 300$ K is imposed across each lamella, the highest temperature is at the boundary between them, the lowest (at the surface of the disc), is that of the quenching medium. Two cases are considered. In the first [Fig. 4(a)], the corners of each plate are allowed to move freely; the conditions at the limits being zero displacement in any direction of the points representing the sticking by the 211 particles. The resulting stress state is symmetric and a slight compressive stress appears on the outer faces. For the second step, a supplementary condition is imposed. Two corners remain in contact [Fig. 4(b)]. It thus corresponds to the introduction of a supplementary 211-particle. The deformation state changes drastically and it can be observed that tensile stresses appear at the coolest (outer) faces. Considering a higher number of inclusions and of the sticking laminates should approach the behaviour of the real textured samples. This is part of on-going work.

4 Conclusion

Composites were made of a textured matrix of the super-conducting ceramic, $\text{YBa}_2\text{Cu}_3\text{O}_x$, and containing particulate dispersions of only the ceramic 211-green phase (up to 60% mol), or 10 and 20% vol, metallic silver, at a 211-content of 60% mol, have been fabricated and tested for toughness and thermal shock resistance. The number of identical samples in the sense of a reproducible microstructure is limited because they are in the stage of research and development. A recently developed approach based on the Vickers indentation technique has thus been put to work. It allows, with the help of a few indentations made on a defined crystallographic plane to determine in a first step the toughness, and in a second the thermal shock resistance. The increase in toughness due to the 211-particles can be additionally increased by the additions of silver-inclusions. It results in a huge increase of the thermal shock resistance, thus making a proof for an optimised superimposition of the effects of silver on both the electrical conductivity⁹ and the thermo-mechanical reliability of functional components and parts. For

the less expensive case of the sole toughening by the 211 inclusions, an apparent discrepancy between the variation of toughness and thermal shock resistance has been noted. Whereas the toughness increases with the increasing amount of the 211 phase, does the thermal shock resistance accordingly decrease. This discrepancy is explained by the competition between the increase in toughness due to the deviation mechanism by the inclusions and that of the maximum thermal stress during quenching which is due to the stiffening effect by the same inclusions. A meso-structural model has been designed for that purpose. Its implementation into a finite element software and calculations shows that the search for the best compromise between super-conducting properties and thermo-mechanical reliability, with respect to the content in the green phase becomes possible.

Acknowledgements

The authors acknowledge the help of J. Wang (Crismat; textured samples) and G. Morice (Leremat; finite element) for their practical contributions to this work.

References

1. Kingery, W. D., Factors affecting the thermal shock resistance of ceramic materials. *J. Am. Ceram. Soc.*, 1955, **38**, 145–155.
2. Buessem, W. R., Thermal shock testing. *J. Am. Ceram. Soc.*, 1955, **38**, 15–17.
3. Tancret, F., Monot, I. and Osterstock, F., Composite effects for increased toughness and thermal shock resistance of sintered YBaCuO ceramic superconductors. *Ann. de Chimie*, 1998, **23**(1–2), 225–228.
4. Tancret, F., Desgardin, G. and Osterstock, F., Influence of porosity on the mechanical properties of cold-isostatically pressed and sintered YBaCuO superconductors. *Phil. Mag. A*, 1997, **75**(2), 503–523.
5. Tancret, F. and Osterstock, F., The Vickers indentation used to evaluate quenching conditions and resistances of brittle materials. *Scripta Mat.*, 1997, **37**(4), 443–447.
6. Chantikul, P., Anstis, G. R., Lawn, B. R. and Marshall, D. B., A critical evaluation of indentation techniques for measuring fracture toughness: II, strength method. *J. Am. Ceram. Soc.*, 1981, **64**(9), 539–543.
7. Cook, R. F., Dinger, T. R. and Clarke, D. R., Fracture toughness measurements of $\text{YBa}_2\text{Cu}_3\text{O}_x$ single crystals. *Applied Physics Letters*, 1987, **51**(6), 454–456.
8. Tancret, F., Elaboration et caractérisation thermo-mécanique de céramiques supraconductrices de type YBaCuO frittées ou texturées. Doctoral Thesis, University of Caen, 1997.
9. Monot, I., Etude physico-chimique de la texturation de céramiques supraconductrices à haute température critique $\text{YBa}_2\text{Cu}_3\text{O}_x$. Doctoral Thesis, University of Caen, 1993.